# Characterization of self-assembled Bis[2-(2-bromoisobutyryloxy) undecyl] disulphide (DBTU) on gold surfaces suitable for use in surface-initiated atom transfer radical polymerization (SI-ATRP)

Miriam Chávez, Laura Fuentes-Rodríguez, Guadalupe Sánchez-Obrero, Rafael Madueño, José Manuel Sevilla*, Manuel Blázquez, Teresa Pineda

*Department of Physical Chemistry and Applied Thermodynamics,*
*Institute of Fine Chemistry and Nanochemistry,*
*University of Cordoba,*
*Campus Rabanales, Ed. Marie Curie 2ª Planta, E-14014 Córdoba, Spain*

# Abstract

Bis[2-(2-bromoisobutyryloxy) undecyl] disulphide (DTBU) is an initiator for surface-initiated atom transfer radical polymerization (SI-ATRP) able to functionalize metal surfaces through formation of self-assembled monolayers (SAM). The goal of this work is the making monolayers with the DTBU initiator on gold polycrystalline electrodes and their study by electrochemical methods as cyclic voltammetry (CV), capacity-potential curves (C-E), electrochemical impedance spectroscopy (EIS), and angle contact measurements for their characterization. Information of the integrity and permeability of the monolayers has been obtained by capacitance-potential measurements and impedance spectra. Also, the blocking effect of the physical barrier that SAM can produce to different redox probes is explored by using voltammetry and impedance. DTBU forms a compact monolayer whose main features are related with heterogeneous chain structures, having a non-polar hydrocarbon internal part and a polar head group. This is confirmed by X-ray photoelectron spectroscopy (XPS) which shows the presence of the elements of the DTBU adsorbate of SAM. Moreover, mixed monolayers of DTBU and 6-mercaptopurine (6MP) have been prepared and characterized, to check if the thiol facilitates electron exchange through monolayers. On this approach, different DTBU:6MP ratios have been employed and characterized studying IRRAS spectra, electrochemical properties, and contact angle on the modified surface. These mixed monolayers provide optimal conditions for adaptation and use in e-ATRP.



**Keywords**: DTBU radical polymerization initiator; self-assembled monolayers; 6-mercaptopurine 6MP; mixed monolayers; cyclic voltammetry; electrochemical impedance spectroscopy; contact angle; XPS; IRRAS.

## 1. Introduction

Atom transfer radical polymerization (ATRP) is one of the polymerization techniques used to produce polymers in a controlled manner [1-5], both from the point of view of the polydispersity and the nature and structure of the final product as copolymers, linear, branched structures, etc. This radical polymerization initiated on a surface (SI-ATRP) providing a way to functionalize a wide variety of substrates with polymers [6]. Its versatility and tolerance towards a wide variety of functional groups has turned this reaction into a synthesis technique widely used to prepare brush polymers [7-11] special relevance due to their applications in the field of nanomedicine [12, 13].

The self-assembled monolayers (SAM) represent a suitable approach to the design of surface chemistry in a wide range of metal substrates since the assembly of small molecules offers a convenient, simple, and highly versatile system to modify the intrinsic properties of the surface [14-17]. Also, properties such as mechanical stability, electrical conductivity, activation potential and reactivity are essential in the initiator bound to the substrate to obtain a good yield and control in the polymerization reaction.

One of the basic objectives of the studies on the formation of a SAM with an initiator molecule for the SI-ATRP, and with electrochemical mediation (e-ATRP), is to find the experimental conditions on the surface where the electronic transfer itself of redox catalyst is facilitated, typically a copper complex with the associated pair Cu(II)/Cu(I) [10, 11]. Li et al., have studied this aspect, after observing that, although short chains seem a good option because of the poorer packaging of SAM that facilitates electronic transfer [18], the polymer growth with these chains is very limited.

On the other hand, chains like those of DTBU (Bis[2-(2-bromoisobutyryloxy) undecyl] disulphide (Scheme 1) inhibit the transfer of the catalyst pair, so the alternative was to assemble a mixed monolayer with a conductive molecule such as 2-thionaphthiol (2-NAT) together with the DTBU [10], obtaining polymer films homogeneous brush. This strategy allowed not only to create charge transfer spaces for the redox reaction through the 2-NAT domains, but also to assemble high quality initiator monolayers for the formation of dense brush-type polymers.

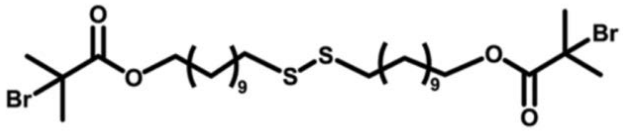


Scheme 1. DTBU molecule

The aim of this work is to obtain functionalized gold surfaces with self-assembled monolayers of initiator of the radical polymerization reaction with atomic transfer (SI-ATRP).

Attention is focused on the determination of the experimental conditions that allow to control the conditioning of the surface. The DTBU molecule is an initiator with the thiol function that allows it to form a self-assembled monolayer on a metal surface, leaving exposed the active center that produces the primary radicals for polymerization.

In this work, polycrystalline gold electrodes were chosen. The characterization of this monolayer by electrochemical methods, contact angle measurements, and XPS and IRRAS, has been performed, where chain interactions play an important role. Also, the formation of mixed monolayers formed with DTBU and 6-mercaptopurine (6MP) has been tested. This last molecule (Scheme 2), has been extensively studied for the formation of self-assembled monolayers on gold and other metallic substrates [19-22], showing that it does not produce blocking effect against molecules such as potassium ferricyanide, except in alkaline medium, due to the formation of a negatively charged monolayer through nitrogen N(9)-H ionization.

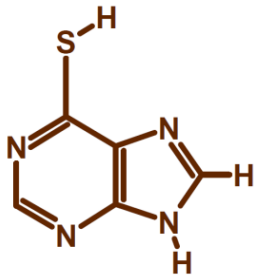


Scheme 2. 6-mercaptopurine molecule

On the other hand, as it has been above reported, the self-assembled DTBU molecule significantly limits the electron transfer by the packing formed on the metallic surface.

Therefore, under the usual experimental conditions, 6MP is a good candidate for the formation of mixed monolayers with DTBU for use in e-ATPR.

## 2. Experimental

### *2.1. Chemicals*

Bis[2-(2-bromoisobutyryloxy) undecyl] disulphide (DTBU), 6-mercaptopurine (6MP), ferrocene-methanol, $K_4Fe(CN)_6$ and $Ru(NH_6)Cl_3$ were from Sigma-Aldrich. Other reagents such as perchloric acid ($HClO_4$, 70%), potassium hydroxide (KOH), ethanol and potassium nitrate ($KNO_3$) were from Merck (analytical quality). All solutions were prepared with deionized water produced by Millipore system.

### *2.2. Methods*

Electrochemical experiments were performed using an Autolab (Ecochemie model Pgstat30) instrument attached to a PC with proper software (GPES and FRA) for the total control of the experiments and data acquisition.

The measurements of electrochemical impedance spectroscopy (EIS) were carried out at different contacted potentials ($E_{dc}$) in a frequency range of 10 kHz to 0.1 Hz and with a potential modulation amplitude (r.m.s.) of 5 mV. The differential capacity-potential curves were obtained by impedance measurements performed at a perturbation frequency f = 49 Hz. The differential capacity was calculated as $C_d = 1/(\omega Z'')$, with Z" being the imaginary part of the total impedance and $\omega = 2\pi f$ being the angular frequency of the perturbation.

For the electrochemical studies Metrohm thermostated electrochemical cells are used under an inert atmosphere of nitrogen, for which this gas was bubbled for 15-20 minutes. A configuration of three electrodes is used. As work electrode (WE) a BAS polycrystalline gold electrode of BioAnalytical System, Kenilworth, UK, of 1.6 mm diameter, or a flat square plate ($1x1cm^2$) of polycrystalline gold, or a gold single crystal with approximately 3-mm diameter and 2-mm thick cylinders with a flat polished side oriented in the (111) surface was used. As auxiliary, a Pt electrode (CE) and a reference electrode (RE) of Ag/AgCl 3M, or a reversible hydrogen electrode (RHE) used for the experiments of determination of the real area. To guarantee the reproducibility of the electrode surface, a treatment was applied. The polycrystalline working electrode was polished with a suspension of $Al_2O_3$ (0.05 μm) in a polisher (Buehler, Metaserv-2000), rinsed and treated with ultrasound in ultra-pure

water for 10 minutes. The surface condition was confirmed by a cyclic voltammogram in 0.01M $HClO_4$, and the real surface area was determined from the stripping reduction peak of oxides and hydroxide on the gold electrode surface [23, 24]. This treatment was the most appropriate for producing a clean and very reproducible surface.

The formation of self-assembled monolayers (SAM) of DTBU, 6MP and mixed DTBU: 6MP were prepared by contacting a fresh clean gold substrate with ethanolic solutions of the mercaptoderivatives at a total concentration of 1 mM, overnight, at room temperature and protected from light. The modified electrodes, once removed from the thiol ethanolic solution, were cleaned by stirring for 15 minutes, or sonicating for 2 minutes, on pure ethanol.

X-ray photoelectronic spectroscopy (XPS) analysis was performed with a SPECS Phoibos 150 MCD spectrometer from SCAI, University of Cordoba, using non monochromatized (12 kV, 300 W) Mg KR radiation (1253.6 eV). The spectra were analyzed following previous reported procedure [25]

*IRRAS characterization.* A 250 nm thick Au layer adhered to a 2.5 nm thin chromium layer deposited on a Borosilicate glass 11×11mm flat surface were used as Au coated substrates (Gold-Arrandee™) for the Infrared Reflection-Absorption Spectroscopy (IRRAS) measurements. IRRA spectra were recorded on a JASCO 6300 FTIR single (He-Ne) laser beam spectrometer in the 400‑4000 $cm^{-1}$ wavenumber range at a resolution of 4 $cm^{-1}$, and the data were acquired by the integrated software (Spectra Manager) [25].

For the determination of the contact angle, an optical Thei tensiometer (Attension, Biolin Scientific) equipped with a high-speed camera (420 fps) was used, with a disposable pipette tip. Milli-Q water was used as measuring fluid. Experimentally, the measurement was made by dropping a constant volume (2μL) onto a solid surface (flat electrode) and recording the image of the drop.

## 3. Results and discussion

### *3.1. Electrochemical characterization*

#### *3.1.1. Reductive desorption (RD) of the DTBU-SAM*

The modification of the gold surface was carried out by self-assembly following the protocol described in the experimental section. The assembly involves the breaking of the S-S bond [16] obtaining a SAM.

Interesting information about SAM properties can be derived by using electrochemical techniques. In this sense, the reductive desorption process (RD) of the molecules bound by an Au-S bond can be monitored by cyclic voltammetry and the electrochemical profile allows an estimation of the DTBU surface coverage according to the equation (1).

$$R{-}S{-}Au + solvent + 1e^{-} \rightarrow Au_{solv} + R{-}S^{-}_{solv} \quad (1)$$

where $Au_{solv}$ and $R\text{-}S^{-}_{solv}$ stand for solvated gold surface and thiolate, respectively. This equation represents a solvent substitution reaction that takes into account the energetic contributions involved in SAMs RD such as substrate-adsorbate, SAM-solvent, lateral interactions, substrate-solvent and surfactant solvation [26]. In this sense, the charge density, should contain not only the faradaic charge due to the RD but also the double layer charging contribution. Moreover, it has been pointed out that although we use the reaction (1) to account for the RD process, the charge flowing to the interface per desorbed molecule is not an integer equal to the number of electron transferred from metal to the molecule but, this value depends on electrode potential and the nature of the supporting electrolyte [27].

Figure 1 (top) shows the I-E curves obtained by cyclic voltammetry (CV) of the reductive desorption of DTBU as well as the blank electrolyte, an aqueous solution of 0.1 M KOH.

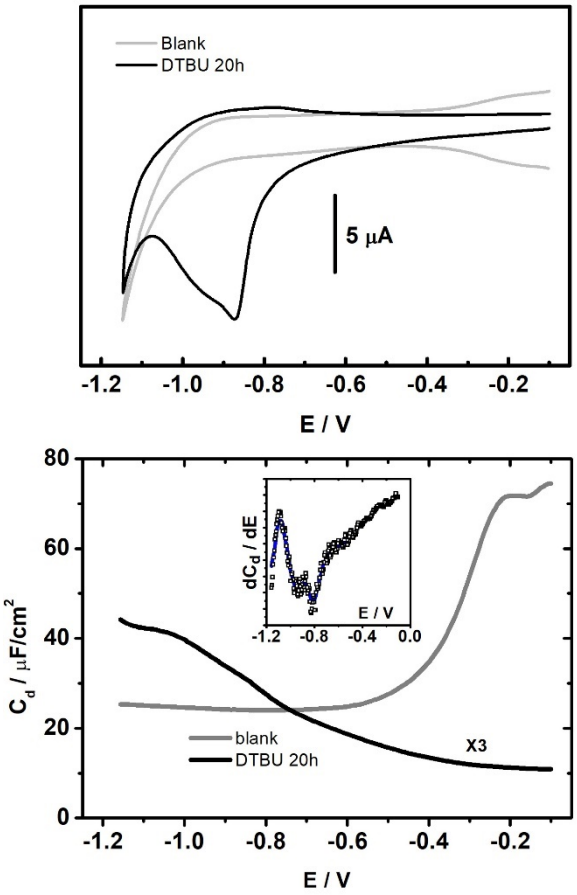


Figure 1. (Top) Voltammogram of the reductive desorption of DTBU monolayer on gold electrode in contact with an aqueous solution KOH 0.1 M. In gray, voltammogram of the bare gold electrode. (Bottom) C-E curves of the reductive desorption of DTBU (Cd x3) and bare electrode (gray). Aqueous solution KOH 0.1 M. frequency 49 Hz. Inset: First derivative of the C-E curve (square). The smoothing operation of the derivative curve (solid line).

The scanning starts at -0.1 V (double layer region), in the cathodic direction to -1.15 V. In this potential interval appears a peak with a shoulder associated to the reductive desorption. A roughly calculation of the surface coverage Γ, by taking into account the charge density obtained under this condition ($\sigma$ = 78.0 μC/cm$^2$), gives a value of 8.1 × 10$^{-10}$ mol·cm$^{-2}$ and an area per DTBU molecule of 21±1 Å$^2$, values that correspond to those of a complete monolayer of aliphatic chain thiols [14]. The calculated results on the surface area of DTBU molecules in SAM from reductive desorption, schematically suggest a typical vertical disposition as in chain alkanethiols according to reference [14] which includes a possible tilt angle with respect to the surface normal. In any case, the arrangement of DTBU on the gold surface is such that it forms a compact monolayer.

The capacitance-potential curves of DTBU/Au have been recorded on 0.1 M KOH solution, under experimental conditions of total surface coverage. Figure 1 (bottom) shows a potential scanning in the direction of the reductive desorption. The great difference between the C-E curve of modified and bare electrode is a decrease in the differential capacity caused by the interaction of DTBU with the polycrystalline gold surface. Also, the C-E curve for the DTBU monolayer in the cathodic potential range shows a profile in which, a gradual and stepped evolution is shown from -0.2 V, suggesting that other processes before RD are observed.

The differential capacity in the potential range -0.1 to -0.2 V is 3.6 $\mu F/cm^2$, a value close to those obtained with alkanethiols with an non-polar hydrocarbon chain which exposed polar terminal groups [28]. It has been tried to improve resolution of the capacitance variation taking its first derivative, curve (inset). The obtained profile indicates that the measurement of capacity potential, unlike the current potential, is sensitive to three transitions in the potential region between -0.4 and -1.0 V. It should be noted that $C_d$ is obtained as $-1/\omega Z''$, so $dC_d/dE$ is the derivative of the inverse of the impedance Z'' (imaginary part), thus sensitive to faradic and non-faradic processes on the electrode surface. The change at more negative potentials where reductive desorption takes place, suggests that the formation of a complete and compact monolayer of DTBU on gold surface involves a strong intermolecular interaction.

*3.1.2. Study of the integrity of DTBU SAM using EIS.*

Electrochemical impedance spectroscopy (EIS) allows to study the electrode-electrolyte interface describing it as an ideal electric double layer (DL), i.e., the Helmholtz model, or whether it deviates due to surface heterogeneity by current leakage at different scale of time [29]. The composition and concentration of the electrolyte may play a role in its behavior, which is often analyzed by the variation of the phase angle with AC polarization frequency. The formation of DTBU monolayers is verified by XPS spectra (Appendix A) in the region of interest confirming the presence of the key elements of the adsorbate-substrate structure (Fig. A1).

Figure 2 shows the Bode plots for the DTBU SAM/Au interface obtained after 20 hours of modification at several DC potentials in the cathodic region. The impedance spectrum for

the bare electrode at -0.2 V (grey line). shows a maximum phase angle close to 80°, which suggests that the polycrystalline gold surface behaves like a non-ideal DL and is represented by a constant phase element (CPE). This might be caused by the intrinsic heterogeneity and surface roughness of the polycrystalline substrate.

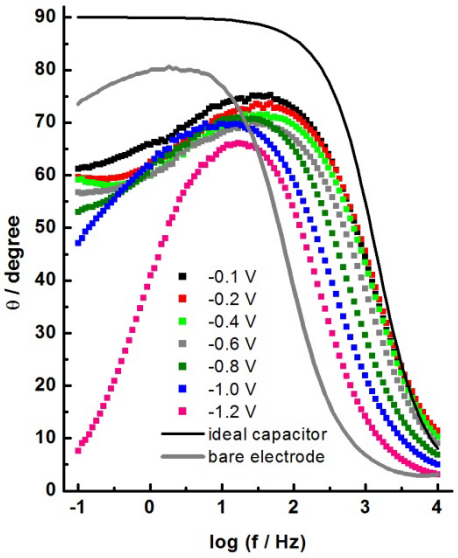


Figure 2. Bode representation of the DTBU-SAM/Au in 0.1 M KOH in the range of potentials from the SAM stability zone, at the least negative edge, to the reductive desorption, at the most negative. Bode representation of the Au(s)/KOH(ac) 0.1M interface (grey). Ideal capacitor (black). Modification time 20 hours.

The theoretical variation of the phase angle with the polarization frequency for an ideal DL is also shown in Fig 2. This simulation assumes a capacitance as that found in the CE curves at less negative potentials, where no faradic response takes place. However, a large deviation from ideal behaviour is observed in the presence of the DTBU film. A maximum phase angle of 70-75º suggests a double layer typical of the solid heterogenous surface. The deviations from ideal capacitive behaviour can be empirically represented by the so-called "constant phase element" (CPE) having the following dependence on frequency and containing the double-layer capacitance quantity, Yo [29]

$$Z(CPE) = 1/(jY_o\omega)^n$$

The parameter n is related to the phase angle θ by $\theta = n(\pi/2)$. n = 1 corresponds to true capacitance behaviour. Moreover, the observed transitions at low frequencies reveal the complexity of this interface. This behaviour suggests that the DTBU chain structure must also be considered. The heterogeneous structure is composed by a non-polar hydrocarbon skeleton inside the SAM and a polar head containing oxygen and bromine atoms. To

understand this complex behaviour as reveals θ-log f curves is necessary to bear in mind that structure, nature, and elements of the DTBU long chain play a main role.

In view of the electrochemical results and considering the structure of the DTBU chain, an equivalent circuit has been selected for the Bode plot fitting, which is appropriate in monolayer with polarity differences on the chains [30, 31]. It allows to obtain information from the Au/DTBU interface. It is a combination of elements in series, Rs(Q1R1), and (Q2R2), with parallel arrangement of the elements enclosed in parentheses. Rs representing the resistance of the solution, and QR an interface with CPE (Q1 and Q2) elements. The (1) and the (2) indexes refer to the surface and inside the monolayer, respectively, where the ions can partially or totally penetrate due to the potential permeability suggested by the electrochemical data. In Scheme 3 a representation of the combination of elements and the configuration of the DTBU monolayer is shown.

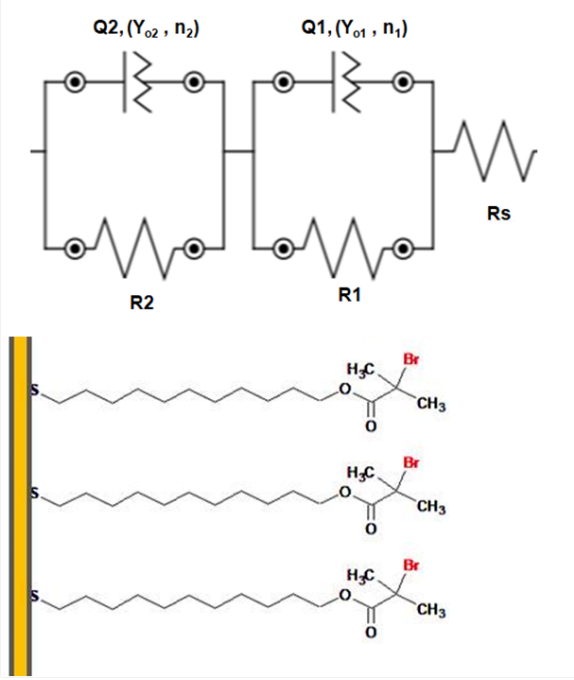


Scheme 3. Equivalent circuit and representation of the DTBU monolayer on polycrystalline gold electrode.

Figure 3 shows the fittings of the Bode-phase curves, under the experimental conditions tested (KOH 0.1 M and $KNO_3$ 0.1 M), according to the equivalent circuit.

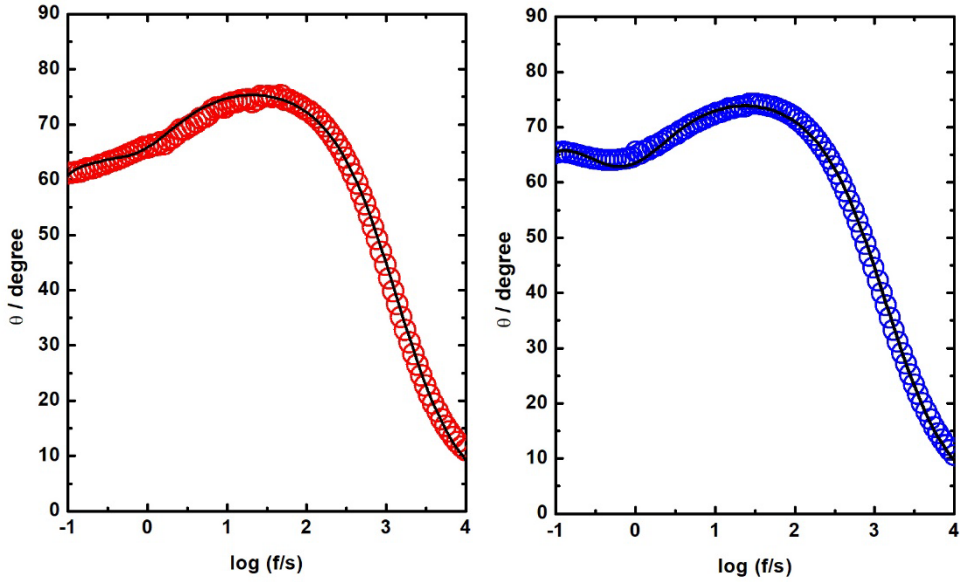


Figure 3. Bode representation and fitting with Rs (R1Q1) (R2Q2). Experimental values (○) equivalent circuit curve (-). Edc = -0.1V. Au/DTBU monolayer in KOH (left) and $KNO_3$ (right) at 0.1M.

An acceptable fitting is obtained which suggests that the interface behaves in agreement with the scheme that considers the structure of DTBU. Other equivalent circuits such as those used in similar systems containing film or porous material on electrode surfaces described in the reference [29] have been tested, showing no improvement in the fit. Table 1 summarizes the results of the parameters obtained in the best fitting.

Table 1. EIS Best Fitting Parameters of the Au/DTBU monolayer in KOH and $KNO_3$ 0.1 M

| **Au/DTBU** | **$R_s$ / $\Omega \cdot cm^2$** | **$Y_{o1} \cdot 10^8$ / $\Omega^{-1/n}s$** | **$n_1$** | **$R_1$ / $k\Omega \cdot cm^2$** | **$Y_{o2} \cdot 10^8$ / $\Omega^{-1/n}s$** | **$n_2$** | **$R_2$ / $k\Omega \cdot cm^2$** |
|---|---|---|---|---|---|---|---|
| **KOH 0.1 M** | 35.0 | 6.32 | 0.8527 | 18.6 | 7.57 | 0.8870 | 593 |
| **$KNO_3$ 0.1 M** | 33.6 | 15.3 | 0.8512 | 7.51 | 16.01 | 0.8663 | 519 |

It is worth noting that the values found for $n_1$ and $n_2$ are consistent with a CPE where the phase angle does not reach 80º in any case. Moreover, $R_1$ and $R_2$ have high values, according to the nature of DTBU being those of $R_2$ which correspond to the hydrophobic inside of the aliphatic chain.

Bode phase curves of the bare electrode show sensitivity on the inflection point at high frequency as compared to the modified substrate. On a first approach, this behaviour can be modelled assuming a simple scheme with an ideal doble layers (DL) that provides a

quantitative relationship between capacitance of bare and modified electrodes at high frequency. For a fixed value of phase angle, $\theta_{1/2}$ would be the ordinate of the inflection point. It can be written

$$f_m(\theta_{1/2})/f_0(\theta_{1/2}) = C_0/C_m$$

Applying to the DTBU SAM interface, the subscripts (o) and (m) refer to the bare gold and modified electrode, respectively. However, if you consider that the interface behaves like a CPE with similar values of n for Au and Au/DTBU, it can be demonstrated that it does not add extra complexity.

In Bode curves of Figure 2, one has analysed the displacement of $f_m(\theta_{1/2})$ with the potential. The determination of $C_m$ from this frequency indicates an almost coincident variation with potential as compared with the differential capacity-potential curves determined by impedance measurements (Table 2).

Table 2. $C_d$ experimental values and $C_m$ calculated values from EIS at different potentials of the Au-DTBU/KOH (ac) 0.1 M interface. $t_{mod}$ = 20 h

| **E / V** | -0.1 | -0.2 | -0.4 | -0.6 | -0.8 | -1.0 | -1.2 |
|---|---|---|---|---|---|---|---|
| **$C_d$ / μF/cm²** | 3.6 | 3.7 | 4.4 | 6.1 | 9.0 | 13.2 | 25.7 |
| **$C_m$ / μF/cm²** | 3.6 | 3.5 | 4.1 | 5.4 | 8.5 | 13.5 | 24.9 |

*3.1.3. Blocking effect of DTBU monolayers*

To examine the blocking properties of the SAM interface of DTBU, a study of several redox probes has been carried out. Therefore, cyclic voltammetry and impedance spectroscopy of $Fe(CN)_6^{3-/4-}$, $Ru(NH_3)_6^{3+/2+}$ and FcMeOH have been employed both with the bare and modified electrodes. It is known that the heterogenous electron transfer of the redox pairs is sensitive to the blockage that occurs on the metal surface with self-assembled monolayers. The observed behavior is able to detect the presence and nature of defects revealing information on the organization of the monolayer [32].

The selected probes show difference in the electrical charge of the reagent molecule (negative, positive, and neutral), and in the nature of the redox pairs and the solvation properties [33, 34]. Figure 4 (left) shows the voltammograms of $Fe(CN)_6^{3-/4-}$ 1 mM in $KNO_3$ 0.1 M onto bare gold electrode, and after 20 h of modification with DTBU. On the right of the Figure 4 is shown EIS (Nyquist plot) in the same experimental conditions. A potential

DC corresponding to the average between the peak potentials of the couple $Fe(CN)_6^{3-/4-}$ was applied.

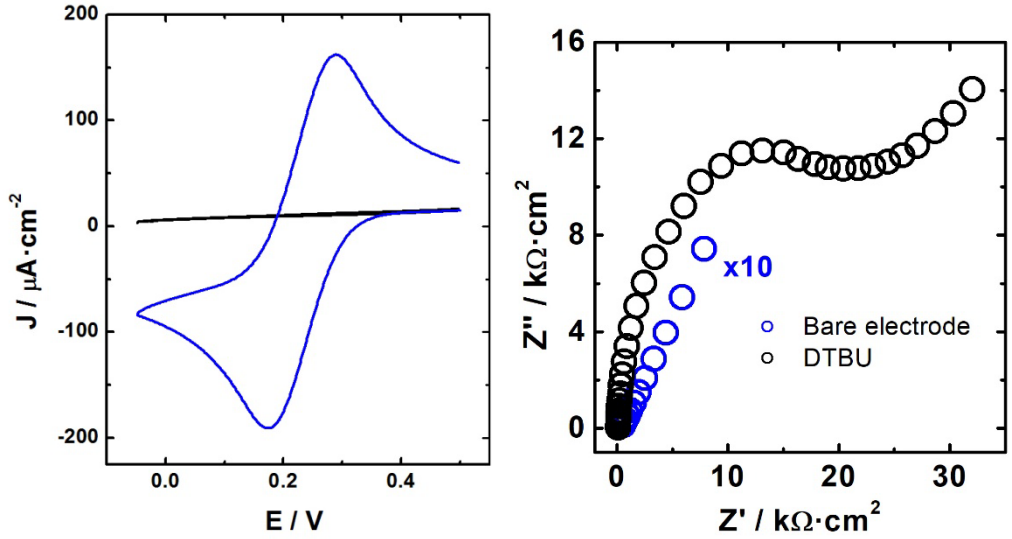


Figure 4. (left) CV of $Fe(CN)_6^{-3/-4}$ 1 mM in $KNO_3$ 0.1 M for bare gold electrode (blue), after 20 h of modification with DTBU (black). Scan rate 0.1 V/s. (right) EIS (Nyquist plot) of $Fe(CN)_6^{-3/-4}$ in the same experimental. $E_{dc}$ = +0.22 V.

With the bare gold electrode, the redox pair is clearly appreciated. The presence of DTBU after 20h of modification gives rise to a total reduction of the current by a blocking effect. The impedance spectra show great sensitivity to the modification of the gold electrode with DTBU. It is observed an arc at high frequency indicative of the appreciable increase of the resistance to the charge transfer in comparison with the bare electrode (Figure 4, right). For $Ru(NH_3)_6^{3+/2+}$ and FcMeOH, no significant changes are observed either in the voltammogram or in the impedance spectrum with respect to the bare electrode (Appendix A).

A Randles circuit has been used with a CPE to model the electric double layer in the fitting of the impedance spectra. The greatest sensitivity to modification of the electrode is highlighted with the $Fe(CN)_6^{3-/4-}$ redox probe where $R_{CT}$ increases by more than two magnitude orders in the presence of DTBU monolayer. The values of n for the modified electrode oscillate between 0.8 and 0.9 assuming a CPE electric double layer.

*3.1.4. Reductive desorption of mixed SAM of DTBU and 6MP.*

The reductive desorption of DTBU-6MP mixed monolayers on the polycrystalline gold electrode in 0.1 M KOH has been studied. The modification was also carried out in ethanol

solutions by using a 1 mM total concentration of thiols and a modification time of 20 h (overnight). The voltammogram of 6MP monolayer has also been recorded under the same experimental conditions for comparison. Figure 5 shows the voltammograms of the RD in the different proportions of modification studied.

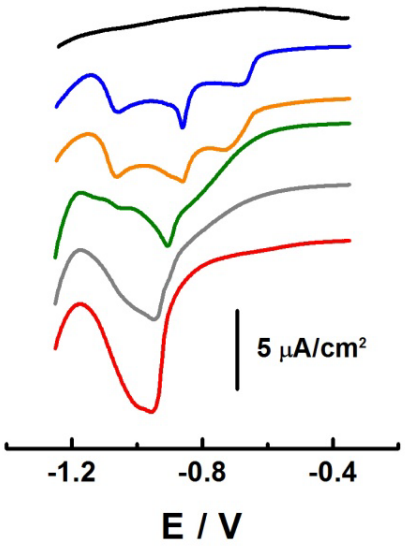


Figure 5. Reductive desorption of the mixed SAM of DTBU and 6MP after 20 h of modification. Scan rate 20 mV/s. Top to bottom: Blank electrolyte; DTBU:6MP ratio: 0:100; 10:90; 30:70; 90:10; 100:0.

The reductive desorption of 6MP has already been studied by our research group [20]. In Figure 5, there are up to three partially overlapped peaks in the RD profile of the 6MP. The approximate peak potentials are -0.67, -0.86 and -1.05 V. These values are close to those obtained with a polyfaceted gold and they matches with those obtained with single crystal facets of Au(111), Au(100) and Au(110), respectively. The onset of the RD faradic current of the 6MP occurs -0.58 V, showing a faradic process extended to negative potentials with a surface charge density of 66±8 $\mu C/cm^2$. The RD profile of DTBU, has already been described in previous sections, the onset is close to -0.75 V and the surface charge density 78±6 $\mu C/cm^2$.

The voltammograms corresponding to the mixtures in the different proportions show an increase of overlapping and a loss of resolution of the peaks, although overall a displacement of the faradic current is observed in the cathode direction as the proportion of DTBU increases. For these mixed monolayers the difficulty for determining the surface charge

density increases, obtaining values that range between 65-70 μC/cm$^2$. This feature indicates that as the proportion of 6MP increases, so does the proportion on the surface of electrode. .

*3.1.5. Study of the integrity and the blocking effect of the mixed layers DTBU:6MP*

IRRAS spectra of mixed DTBU:6MP monolayers have been recorded (Appendix A), indicating that 6MP is present in a significant proportion on the surface as expected from the modifying mixture. The bands assigned to the C-N stretching mode of the 6MP rings stand out in the spectrum, at 1690 cm$^{-1}$ which is a clear indicator of the interaction of 6MP with the gold surface (appendix A). The integrity of the mixed monolayers has been studied through EIS and analyzed from the Bode phase representation. Figure 6 shows the impedance spectra θ-log f for 6MP, DTBU and selected mixtures for $E_{dc}$ = 0.0 V. Similar results have been found at potentials -0.2, -0.1, +0.1 and +0.2 V.

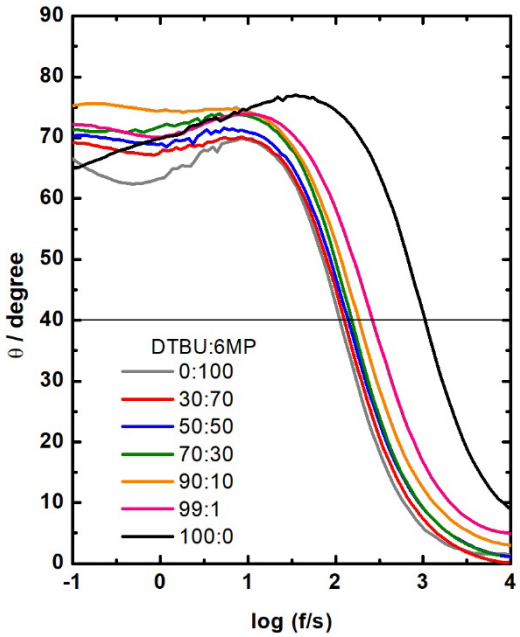


Figure 6. Bode plot for DTBU, 6MP and DTBU:6MP ratio 30:70, 50:50, 70:30, 90:10 y 99:1. $E_{dc}$ = 0.0 V.

All the spectra have a profile with the characteristic displacement of the inflection point as those obtained for DTBU. It is observed that for 6MP SAM the value of f($\theta_{1/2}$) at high frequencies (2.04) takes place a decade below of that to DTBU (3.04). On the other hand, for the different ratio, this parameter gradually moves to higher frequencies as the amount of DTBU increases. The figure shows a horizontal line that marks the angle 40º, the same

reference as when the comparison between the differential capacity of the bare electrode versus the modified electrode with DTBU was made. If we accept the capacity-frequency relationship as in the previous case, we can write the relation $C_{m1}/C_{m2} = f_{m2}/f_{m1}$, where $m_1$ and $m_2$ are the symbols used for the two monolayers to be compared. In mixed monolayers, a model with a parallel combination of the differential capacity to each SAM is used, so that the total capacity is the sum of the individual contribution weighted by the number of molecules of each on the surface [34]. Thus, it can be written:

$$C = \chi_{DTBU} \cdot C_{DTBU} + \chi_{6MP} \cdot C_{6MP}$$

where $C_{DTBU}$ and $C_{6MP}$ are the capacitances of pure DTBU and 6MP SAM, respectively. Considering the binary mixture on the surface, with $\chi_{DTBU} + \chi_{6MP} = 1$, and combining with the previous equations, an expression is reached that allows to estimate the composition at the interface:

$$\chi_{6MP} = \frac{f_{6MP}}{f} \frac{(f_{DTBU} - f)}{(f_{DTBU} - f_{6MP})}$$

whit f being the value of $f(\theta_{1/2})$ for any given mixed monolayer of DTBU and 6MP and the rest of symbols having its usual meaning. Under the modification conditions of the gold electrode with both molecules, the proportion of 6MP onto electrode surface is higher than that of modification mixture in all cases. This is suggested by the low gradual displacement of $f(\theta_{1/2})$ that can be observed in Figure 6.

*3.2. Contact angle measurements*

The hydrophilic/hydrophobic character of the DTBU-SAM and mixed monolayers with 6MP has been studied by contact angle (CA) measurements. The variation of the contact angle with the 6MP composition in solution is shown in Figure 7. The representation is practically linear, which would be in accordance with a surface composition like that of the solution mixture, and which is in accordance with Cassie model [35], which indicates that there is no selective fixation (attachment) from one of the thiols.

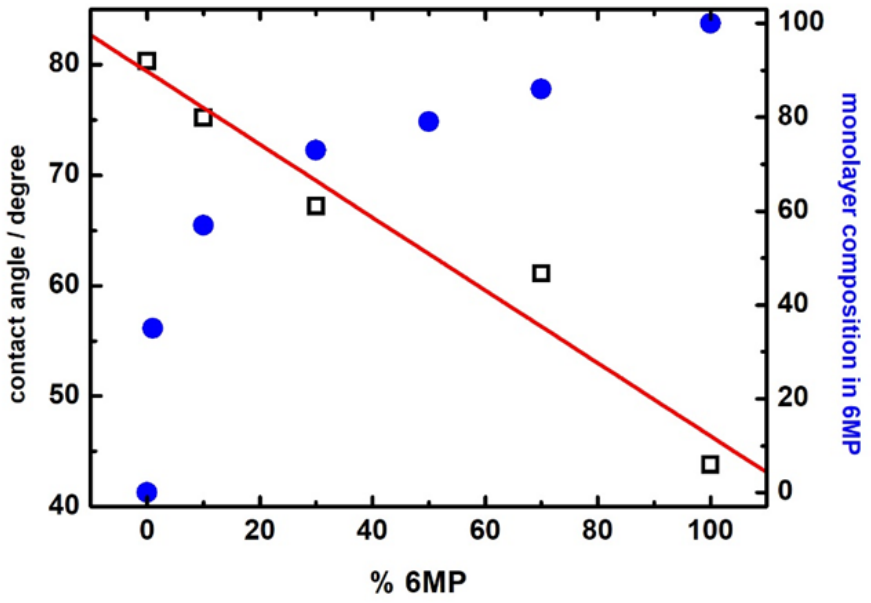


Figure 7. Contact angle on DTBU and 6MP monolayers and mixed monolayers DTBU:6MP in different ratios. (□) experimental CA; (—) Linear Fit; (●) % 6MP on the surface.

However, this interpretation is in marked contrast what was observed by EIS that suggests the preferential binding of 6MP over DTBU and considering this behaviour, it is possible to label the surface composition of the mixed SAM that give rise the cyclic voltametric profiles (Figure 5). This is also in agreement with the significative perturbation of the IR spectrum in the presence of a small proportion of 6MP in the thiol mixture (Figure A2-C). Figure 7 compares the surface concentration of 6MP with the proportion in solution being able to appreciate this fact. This type of deviation has been explained in terms of the formation of random surface structures, without domain location, and solvation differences of exposed heads to the medium (water). The lower proportion of DTBU on the surface is compensated by the predominance of the hydrophobic effect [16, 36] , which due to the larger size limits water access to 6MP (Scheme 4). This behavior results on an apparent proportionality between contact angle and composition in solution as observed in the figure.

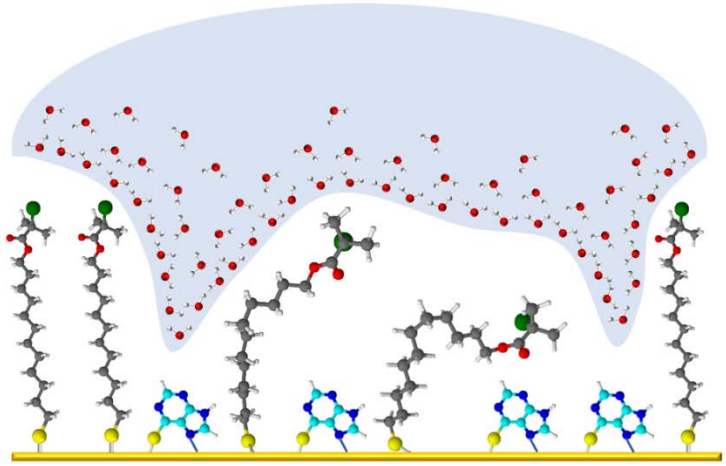

Scheme 4. Mixed monolayer DTBU:6MP. Limitation of access to water and hydrophobic effect.

The collected results suggest examining the conductive properties of the mixed SAMs. Accordingly, the blocking effect of DTBU:6MP monolayers, against the $Fe(CN)_6^{3-/4-}$ redox probe has been explored, for possible changes in the rate of the electron transfer. Figure 8 shows the impedance spectrum of the redox probes on a mixed monolayer 90:10 as compared to that obtained with bare electrode and of the DTBU and 6MP monolayers.

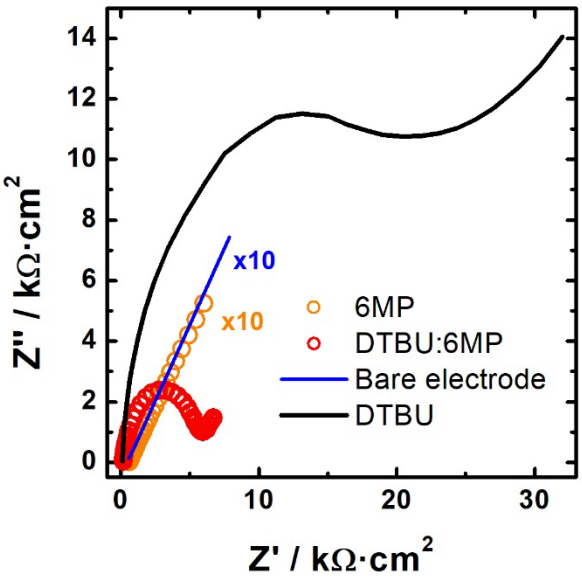


Figure 8. EIS (Nyquist plot) of $Fe(CN)_6^{-3/-4}$ 1 mM in $KNO_3$ 0.1 M for bare gold electrode (blue), self-assembled monolayer with DTBU (black), SAM with 6MP (orange) and mixed monolayer DTBU:6MP from a ratio 90:10 in solution (red). $E_{dc}$ = +0.22 V.

A semicircle at high frequencies is observed which indicates that the resistance to electron transfer is higher than to the bare electrode, although it is much lower than that obtained with the DTBU monolayer.

However, for a 6MP SAM, no appreciable differences are observed with respect to the bare electrode, highlighting the diffusion line in the entire frequency range. Considering a Randles circuit, a very low value of Rct, 0.010 kΩ, is obtained by fitting. This feature suggests the choice of this molecule in the preparation of mixed monolayers to activate the DTBU response as an initiator

The value obtained for the resistance to charge transfer for a mixed monolayer DTBU: 6MP is 0.791 kΩ, clearly higher than the obtained value either with a bare electrode (0.031 kΩ) and with an Au-6MP, but it is lower by a factor to 8 with respect to that corresponding to the DTBU monolayer. This last result shows that the presence of 6MP increases the rate of the electronic transfer of redox couple such as $Fe(CN)_6^{3-/4-}$ and, therefore, the DTBU-6MP mixed monolayer provide the optimal conditions for its adaptation and use in e-ATPR.

**4. Conclusions**

DTBU, initiator in ATRP polymerization reactions, forms self-assembled monolayers on Au substrates through the S-Au bond as it is confirmed by XPS. The peaks associated to the reductive desorption of the SAM (for $t_{MOD}$ overnight) is coherent with a compact monolayer with a molecule footprint of 20.5 $Å^2$. The C-E curves support this characterization, with a differential capacity of 3.6 $\mu F/cm^2$ for the SAM. In consequence, DTBU is postulated as a good candidate to be an initiator in SI-ATRP.

The studies on the integrity of DTBU on polycrystalline gold reveal the presence of a film whose characteristics are defined by a non-polar site near the surface and a polar character by exposed groups to the solution. The phase angle at high frequency is sensitive to the dielectric properties of the electric double layer of the modified electrode, establishing an excellent correlation between transition frequency $f(\theta_{1/2})$ and differential capacity. At low frequencies, variations dependent on the potential are observed which suggest a certain permeability of formed SAMs. The $Fe(CN)_6^{3-/4-}$ redox probe suffers a significative limitation in the electron transfer by the presence of a DTBU compact monolayer.

The IRRAS studies of mixed monolayers DTBU:6MP, indicate that 6MP is present in higher proportion on the surface as expected from the modification mixture. The bands assigned to the C-N stretching mode of the 6MP rings stand out in the spectrum, at 1690 $cm^{-1}$ that is a clear indication of the interaction of 6MP with gold surface. For a 90:10 ratio, the estimated proportion of 6MP on the electrode surface by frequency transition $f(\theta_{1/2})$ in EIS measurements, exceeds that of DTBU. In this mixed monolayer, the $Fe(CN)_6^{3-/4-}$ probe has a charge transfer resistance an order of magnitude lower that the corresponding to the DTBU monolayer. This feature provides optimal conditions for its adaptation and use in e-ATRP.

DTBU and DTBU-6MP SAMs contact angle measurements suggest the formation of random structures on the surface. The differences in the solvation of the exposed heads to the environment (water), leads to a more hydrophobic predominant effect, providing conditions that also favor radical polymerization on the electrode surface.

**Acknowledgements**

We thank the Ministerio de Ciencia e Innovación (Project RED2018-102412-T Network of Excellence Electrochemical Sensors and Biosensors), Junta de Andalucía and Universidad de Cordoba (UCO-FEDER ref. 1265074-2B and Plan Propio, Submod. 1.2.) for financial support of this work. M.C. acknowledges Ministerio de Universidades for FPU 17/03873 grant.

## 5. References

[1] J.S. Wang, K. Matyjaszewski, Controlled Living Radical Polymerization - Atom-Transfer Radical Polymerization in the Presence of Transition-Metal Complexes, J. Am. Chem. Soc. 117(20) (1995) 5614-5615.

[2] M. Kato, M. Kamigaito, M. Sawamoto, T. Higashimura, Polymerization of Methyl-Methacrylate with the Carbon-Tetrachloride Dichlorotris(Triphenylphosphine)Ruthenium(II) methylaluminum Bis(2,6-Di-Tert-Butylphenoxide) Initiating System - Possibilityof Living Radical Polymerization, Macromolecules 28(5) (1995) 1721-1723.

[3] V. Percec, B. Barboiu, Living Radical Polymerization of Styrene Initiated by Arenesulfonyl Chlorides and Cu-I(BPY) (N)Cl, Macromolecules 28(23) (1995) 7970-7972.

[4] R. Barbey, L. Lavanant, D. Paripovic, N. Schuwer, C. Sugnaux, S. Tugulu, H.A. Klok, Polymer Brushes via Surface-Initiated Controlled Radical Polymerization: Synthesis, Characterization, Properties, and Applications, Chem. Rev. 109(11) (2009) 5437-5527.

[5] J.O. Zoppe, N.C. Ataman, P. Mocny, J. Wang, J. Moraes, H.A. Klok, Surface-Initiated Controlled Radical Polymerization: State-of-the-Art, Opportunities, and Challenges in Surface and Interface Engineering with Polymer Brushes (vol 117, pg 1105, 2017), Chem. Rev. 117(5) (2017) 4667-4667.

[6] S. Edmondson, V.L. Osborne, W.T.S. Huck, Polymer brushes via surface-initiated polymerizations, Chem. Soc. Rev. 33(1) (2004) 14-22.

[7] K. Matyjaszewski, P.J. Miller, N. Shukla, B. Immaraporn, A. Gelman, B.B. Luokala, T.M. Siclovan, G. Kickelbick, T. Vallant, H. Hoffmann, T. Pakula, Polymers at interfaces: Using atom transfer radical polymerization in the controlled growth of homopolymers and block copolymers from silicon surfaces in the absence of untethered sacrificial initiator, Macromolecules 32(26) (1999) 8716-8724.

[8] W.X. Huang, J.B. Kim, M.L. Bruening, G.L. Baker, Functionalization of surfaces by water-accelerated atom-transfer radical polymerization of hydroxyethyl methacrylate and subsequent derivatization, Macromolecules 35(4) (2002) 1175-1179.

[9] K. Matyjaszewski, H.C. Dong, W. Jakubowski, J. Pietrasik, A. Kusumo, Grafting from surfaces for "Everyone": ARGET ATRP in the presence of air, Langmuir 23(8) (2007) 4528-4531.

[10] B. Li, B. Yu, W.T.S. Huck, F. Zhou, W.M. Liu, Electrochemically Induced Surface-Initiated Atom-Transfer Radical Polymerization, Angew. Chem.-Int. Ed. 51(21) (2012) 5092-5095.

[11] B. Li, B. Yu, W.T.S. Huck, W.M. Liu, F. Zhou, Electrochemically Mediated Atom Transfer Radical Polymerization on Nonconducting Substrates: Controlled Brush Growth through Catalyst Diffusion, J. Am. Chem. Soc. 135(5) (2013) 1708-1710.

[12] M. Mullner, Molecular Polymer Brushes in Nanomedicine, Macromol. Chem. Phys. 217(20) (2016) 2209-2222.

[13] M. Mullner, K. Yang, A. Kaur, E.J. New, Aspect-ratio-dependent interaction of molecular polymer brushes and multicellular tumour spheroids, Polymer Chem. 9(25) (2018) 3461-3465.

[14] F. Schreiber, Structure and growth of self-assembling monolayers, Prog. Surf. Sci. 65(5-8) (2000) 151-256.

[15] J.C. Love, L.A. Estroff, J.K. Kriebel, R.G. Nuzzo, G.M. Whitesides, Self-assembled monolayers of thiolates on metals as a form of nanotechnology, Chem. Rev. 105(4) (2005) 1103-1169.

[16] E. Albayrak, S. Karabuga, G. Bracco, M.F. Danisman, 11-Hydroxyundecyl octadecyl disulfide self-assembled monolayers on Au(111), Appl. Surf. Sci. 311 (2014) 643-647.

[17] S.M. Flores, A. Shaporenko, C. Vavilala, H.-J. Butt, M. Schmittel, M. Zharnikov, R. Berger, Control of surface properties of self-assembled monolayers by tuning the degree of molecular asymmetry, Surf. Sci. 600(14) (2006) 2847-2856.

[18] J.J. Gooding, F. Mearns, W.R. Yang, J.Q. Liu, Self-assembled monolayers into the 21(st) century: Recent advances and applications, Electroanalysis 15(2) (2003) 81-96.

[19] T. Pineda, J.M. Sevilla, A.J. Roman, R. Madueno, M. Blazquez, Modification of metal substrates and its application to the study of redox proteins, Stability and Stabilization of Biocatalysts 15 (1998) 697-702.

[20] R. Madueno, J.M. Sevilla, T. Pineda, A.J. Roman, M. Blazquez, A voltammetric study of 6-mercaptopurine monolayers on polycrystalline gold electrodes, J. Electroanal. Chem. 506(2) (2001) 92-98.

[21] R. Madueno, D. Garcia-Raya, A.J. Viudez, J.M. Sevilla, T. Pineda, M. Blazquez, Influence of the solution pH in the 6-mercaptopurine self-assembled monolayer (6MP-SAM) on a Au(111) single-crystal electrode, Langmuir 23(22) (2007) 11027-11033.

[22] J.M. Sevilla, T. Pineda, R. Madueno, A.J. Roman, M. Blazquez, Characterization of 6-mercaptopurine monolayers on Hg surfaces, J. Electroanal. Chem. 442(1-2) (1998) 107-112.

[23] S. Trasatti, O.A. Petrii, Real Surface-area Measurements in Electrochemistry, Pure Appl. Chem. 63(5) (1991) 711-734.

[24] M. Lukaszewski, M. Soszko, A. Czerwinski, Electrochemical Methods of Real Surface Area Determination of Noble Metal Electrodes - an Overview, Int. J. Electrochem. Sci. 11(6) (2016) 4442-4469.

[25] M. Chávez, G. Sánchez-Obrero, R. Madueño, J.M. Sevilla, M. Blázquez, T. Pineda, Characterization of a self-assembled monolayer of O-(2-Mercaptoethyl)-O′-methyl-hexa(ethylene glycol) (EG7-SAM) on gold electrodes, J. Electroanal. Chem. 880 (2021) 114892.

[26] R.C. Salvarezza, P. Carro, The electrochemical stability of thiols on gold surfaces, J. Electroanal. Chem. 819 (2018) 234-239.

[27] T. Laredo, J. Leitch, M.H. Chen, I.J. Burgess, J.R. Dutcher, J. Lipkowski, Measurement of the charge number per adsorbed molecule and packing densities of self-assembled long-chain monolayers of thiols, Langmuir 23(11) (2007) 6205-6211.

[28] A.R. Puente-Santiago, G. Sanchez-Obrero, T. Pineda, M. Blazquez, R. Madueno, Influence of Patterning in the Acid-Base Interfacial Properties of Homogeneously Mixed CH3- and COOH-Terminated Self-Assembled Monolayers, J. Phys. Chem. C 122(5) (2018) 2854-2865.

[29] B.E. Conway, Impedance Behavior of Electrochemical Supercapacitors and Porous Electrodes, in: E. Barsoukov, J.R. Macdonald (Eds.), Impedance Spectroscopy: Theory, Experiment, and Applications, 2nd Edition, Wiley, New Jersey, 2005, pp. 495-496.

[30] S. Gritsch, P. Nollert, F. Jahnig, E. Sackmann, Impedance spectroscopy of porin and gramicidin pores reconstituted into supported lipid bilayers on indium-tin-oxide electrodes, Langmuir 14(11) (1998) 3118-3125.

[31] A.E. Vallejo, C.A. Gervasi, Impedance analysis of ion transport through gramicidin channels in supported lipid bilayers, Bioelectrochemistry 57(1) (2002) 1-7.

[32] E. Boubour, R.B. Lennox, Insulating properties of self-assembled monolayers monitored by impedance spectroscopy, Langmuir 16(9) (2000) 4222-4228.

[33] T. Doneux, A. de Ghellinck, E. Triffaux, N. Brouette, M. Sferrazza, C. Buess-Herman, Electron Transfer Across an Antifouling Mercapto-hepta(ethylene glycol) Self-Assembled Monolayer, J. Phys. Chem. C 120(29) (2016) 15915-15922.

[34] G. Sanchez-Obrero, M. Chavez, R. Madueno, M. Blazquez, T. Pineda, J.M. Lopez-Romero, F. Sarabia, J. Hierrezuelo, R. Contreras-Caceres, Study of the self-assembly process of an oligo(ethylene glycol)-thioacetyl substituted theophylline (THEO) on gold substrates, J. Electroanal. Chem. 823 (2018) 663-671.

[35] A.B.D. Cassie, Contact Angles, Discussions of the Faraday Society 3 (1948) 11-16.

[36] Y.J. Liu, N.M. Navasero, H.Z. Yu, Structure and reactivity of mixed co-carboxyalkyl/alkyl monolayers on silicon: ATR-FTIR spectroscopy and contact angle titration, Langmuir 20(10) (2004) 4039-4050.